Research Article

Investigation of feed-forward back propagation ANN using voltage signals for the early prediction of the welding defect

Dinu Thomas Thekkuden[1] · Abdel-Hamid Ismail Mourad[1,2]

© Springer Nature Switzerland AG 2019

Abstract

The research paper investigates the prediction capability of the artificial neural network for weld quality assessment from the captured voltage signals in a gas metal arc welding process. The bead-on-plate welds and v-groove welds were made on SA 516 grade 70 material by altering different parameters such as stickout distance, gas flow rate and travel speed. The voltage signals of each weld were captured using a data acquisition system having 8000 Hz data acquisition rate. The descriptive statistics of the voltage data such as mean, standard error, median, mode, standard deviation, sample variance, kurtosis, skewness, minimum and maximum corresponding to bead-on-plate welds and v-groove welds were used for training and testing the neural network respectively. The quality of the weld was assessed by the visual inspection, and from control charts plotted using voltage data. Overall classification accuracy of 94.7% was achieved in the training process. The feed-forward back propagation neural network predicted the quality of test v-groove welds accurately with a 90.9% prediction rate. The results proved that the developed method is promising for the immediate and early prediction of the weld quality.

Keywords Weld quality · Artificial neural network · Fast-forward back propagation · Welding voltage

1 Introduction

Gas metal arc welding (GMAW) process is widely chosen for joining thick parts due to their inherent ability of high deposition rate. The quality of the weld is a predominant factor in providing strength to the final structure. The presence of a defect is not expected in the welding process due to their ability to degrade the joint strength. Any failure in determining the defects during the manufacturing process or service inspection could cause catastrophic failure without any warning at operating conditions. The welding parameters have a crucial role in the production of quality defect-free weld joints. Commonly observed weld defects in gas metal arc welding are burnthrough, lack of fusion, undercutting, porosity, voids, spatters and whiskers. Regular inspection is advised for equipment, such as pressure vessel, boilers, steam generators, etc., which operate at high pressure and temperature. For the same reason, novel methodologies for failure prevention are encouraged in the present industrial practices. Therefore, owing to vital importance, gas metal arc welding of SA 516 material, which is widely used in pressure vessels and boilers, and the scope of the artificial neural network for the identification of the weld quality are experimentally evaluated in the current research.

✉ Abdel-Hamid Ismail Mourad, ahmourad@uaeu.ac.ae | [1]Mechanical Engineering Department, College of Engineering, United Arab Emirates University, P.O. Box 15551, Al-Ain, United Arab Emirates. [2]Mechanical Design Department, Faculty of Engineering, El Mataria, Helwan University, Cairo, Egypt.

Potential innovations for real-time monitoring were proposed in the past to evaluate the quality of the weld in the last decade. The extracted information from the welding sound, voltage signals, current signals, power, weld-pool image, arc spectrum intensity correlates with welding quality [1]. Many methodologies were suggested to detect faults and weld quality. It was found that the Mahalanobis distance calculated from normally distributed welding current and voltage values was sensitive to defects. The welding quality tester (WQT), developed based on Mahalanobis distance technique, was successful in quantifying the welding quality [2]. The cracks embedded in the material will affect the mechanical characteristics of the material [3–6]. The imperfect fusion and splash in a resistance spot welding can be detected as a part of a quality assessment by monitoring the parameters such as voltage, current, electrode displacement and electrode pressure [7]. An automated vision-based inspection system with the aid of image processing technique was found to detect the presence and position of the undercut defect in a shell-tube weld [8]. The weld image contains geometrical and textural features. The welding quality was determined from the weighted weld strength, elongation, bending angle and impact energy. The back propagation neural network model based on welding quality and weld image was established to monitor the welding quality instantly [9]. For the case of resistance spot welding, the current parameter has a predominant influence in the nugget size and the quality of the weld. The resistance to the current has a remarkable role in all the resistance welding processes. It is known that the overall resistance decreases with the increase in the current value; therefore, dynamic resistance variation during the process is expected to reveal the characteristics of the weld quality. The back-propagation neural network was found to be more reliable than the multiple linear regression for monitoring welds [10]. The mean temperature, strain and strain rate were found out at the reference nodes selected while simulating the linear friction welding (LFW) performed using the parameters such as frequency, pressure, amplitude and time. The three outcomes and pressure were fed to the neural network as inputs to classify the condition of the weld. The results proved the neural network considered to be effective in predicting the occurrence of solid bonding [11]. In fact, the welding techniques have to be chosen carefully to meet the operating conditions and requirements. Laser beam welding with optimized parameters was found to impart corrosion resistance compared to gas metal arc welding using the same material [12]. The defects in a weldment affects the mechanical and metallurgical characteristics irrespective of the welding techniques [13, 14]. The heat distributed across the weld affects the fracture toughness. The cracks present in the parent metal or weld region usually grow due to the applied load [15–17]. Therefore, there is a vast scope for further exploring the methodologies using any potential sources for weld inspection.

The welding voltage is an important parameter in many of the welding processes. The electrode voltage in small-scale resistance spot welding which correlates with welding current, dynamic resistance and nugget formation can be used effectively for investigating the weld quality of titanium welds. The voltage curve plotted for each of the welding processes for definite electrode load, or welding current has been divided into four stages. The Generalized regression neural network (GRNN) model with extracted inputs, such as end voltage of each stage, time, period, variation of the voltage, and mean voltage change rate, was found to be useful in determining the failure load and level of weld quality [18]. Welding voltage and light signals can be referred to identify the stages in the droplet transfer mode due to their superior capabilities. For example, welding voltage is more reliable and efficient than light emissions in distinguishing the welding detachments during streaming, spray, globular modes and at peak or background current detachments [19]. The voltage waveforms are found to be more significant in the process description and the assessment of arc stability in shielded electrode welding process [20]. The investigation for the prediction of the weld quality in a pulsed metal inert gas welding using radial basis function network and back propagation neural network indicated that the statistical parameters of welding parameters are the most significant input data; having a major impact compared to the welding parameters alone [21]. The control chart and probability density distribution plotted using the voltage values can be deployed for finding the presence of the porosity and location. The voltage-based control chart is efficient enough to detect internal minute porosities. The voltage variation upon arc disturbance is the underlying principle for defect detection [22, 23]. The linear discriminant analysis with universal predictor group compromising voltage, wire feed speed, and the power spectral density components of arc current at 0 Hz and between 20 to 40 Hz predicted the weld quality based on the presence of the porosity accurately [24]. Research with different outlooks has been conducted in the past to determine the effect of process parameters especially current and voltage upon arc disturbances. Some of the statistical parameters of current and voltage are found to have significant variations in the regions having large holes made in the welding direction intentionally. A monitoring system based on control charts from the voltage proved to have 100% identification rate for the normal condition and 95% identification rate for the abnormal condition. C.S Wu et al. [25] found out that the statistical parameters

such as mean, coefficient of variation, standard deviation and kurtosis of welding voltage; mean, kurtosis and coefficient of variation of welding current considerably changed during the process disturbance. These considerable changes in the characteristic variable during the arc disturbance motivated to choose the whole statistical description of the welding voltage for the present study.

Several intelligent models with high computational ability were introduced in the past years for operations such as classification, optimization, pattern recognition, clustering, and fitting. Artificial intelligence, being the research interest in the area of robotics nowadays, has a huge impact on equipping machines with perception. The machine learning algorithms were depended widely for the prediction of the response variable in the various multidisciplinary analysis. The extraction of useful information from raw data is difficult without proper methodology and vision. To succeed in data collection, mining algorithms develop a model following 3 stages. In the first stage, the algorithms search for any specific trend or pattern. Then, the second stage defines the parameters that will be utilized based on the results obtained from the first stage. The final stage extracts useful information by applying the defined parameters to the entire set of data. In many of the studies, the parameters of the manufacturing processes were independent variables that were used for training the algorithms. The ultimate tensile strength of the friction stir welded joints were predicted from the fed parameters such as spindle speed, plunge force, and welding speed [26]. The power, focal diameter, and radiation time of the thermal-based process that used Gaussian heat source were sufficient to determine the unknown heat affected zone and temperature using hybrid genetic algorithm-artificial neural network (GA-ANN) model [27]. In a gas metal arc welding process with CMT metal transfer mode, the bead characteristics such as bead width, bead height, penetration depth, and dilution area were predicted using the welding speed, peak welding current and heat input [28]. In many of the experiments, the error associated with the artificial neural network was less compared to other models, although it depends on the application and the data associated with. The study comparing the artificial neural network and multiple regression analysis for predicting the heat affected zone and bead dimensions from altered wire feed rate, stick-out distance, and transverse speed proved to have better accuracy for the former model [29]. The validation of the predicted values is necessary for checking the adequacy of the model. Experimental, numerical, and analytical techniques are commonly preferred for the validation of the developed models using machine learning algorithms. The data mining algorithms were integral parts of artificial intelligent monitoring systems.

Data mining algorithms were used previously for fault analysis applicable to various applications. Data analysis using machine learning algorithms has been effectively conducted using data collected from welding voltage, welding current, radiographic films images, ultrasonic images, infrared thermal images, acoustic data, 3D weld image, etc. A table showing the accuracy achieved in these research investigations are given in Table 1. A range of accuracy from 62.5 to 97.2% is observed for monitoring the weld quality and classification of the defects using several data mining algorithms. According to reported literature, accuracy attained solely by neural networks using different data sources from 78.9% onwards are satisfactory. However, high classification accuracy such as 97.2% and 95% are advantageous compared to those falling in the range between 78.9 and 90% as reported in Table 1.

There are several learning methods and variants for developing neural network models. Gradient descent, scaled conjugate gradient (SCG) and Levenberg–Marquardt (LM) are some of well-known learning algorithms. Scaled conjugate algorithm is proven for fast supervised learning that needs no critical user- dependent parameters and less time [30, 31]. However in most of the several applications, LM is observed to be more efficient than SCG in terms of accuracy whereas, SCG requires less data processing time [32, 33]. On the contrary, SCG is also found to be accurate for certain analysis conducted [34]. Therefore, the suitability of learning algorithms depends on the dataset and other training parameters. A comparative study of learning algorithms in ANN in the field of weld quality inspection is very lacking. Henceforth, SCG is investigated in this current research as an initial evaluation.

The ANN developed by extracting the data from different sources were successfully used previously for predicting various responses. However, novel methods using ANN for determining the quality of the weld to replace the traditional non-destructive tests are rare. Therefore, the possibility of an ANN model using voltage information from the bead-on-plate trial welds for checking the weld quality of real joint (V-groove joint) is investigated in this research. Bead-on-plate trial welds are the welds performed over a plate with an intention to determine the appropriateness of the electrode on the base material and also to estimate the bead characteristics corresponding to the set welding parameters. In real practice, bead-on-plate trials are followed by joint welds. This study is aimed to develop an ANN for predicting the quality of the weld joints from bead-on-plate welding trails. Therefore, the present research is unique in the area of fault analysis and can be easily implemented for a quick inspection. The model was concluded to be widely adaptable with less time consumption and better accuracy compared to non-destructive tests.

Table 1 Accuracy of data mining algorithms in welding fault analysis from literature

Algorithm	Data source	Objective	Welding process	Accuracy (%)
Fuzzy Kohonen clustering network	Welding current	Development of a real-time monitoring system based on current transients.	Gas metal arc welding [35]	90
Decision tree	Current	Classification of weld defects	Gas metal arc welding [36]	94.44
	Voltage			96.83
Naïve Bayes	Acoustic signals	Monitoring of the weld quality	Shielded metal arc welding [37]	62.5
Support Vector Machines				67.96
Neural Network				82.76
J48	Acoustic signals	Classification of weld defects	Shielded metal arc welding [38]	70.78
Random Forest				88.69
Neural Network [39]	Radiographic image	Classification of weld defects	Not specified	80
Adaptive network based fuzzy inference system	Radiographic image	Classification of weld defects	Not specified	82.6
Artificial Neural Network [40]				78.9
Artificial Neural Network [41]	Magnetic Flux Leakage	To classify defected and non-defected pipe welds	Not specified	94.2
Cascade Feed Forward Back Propagation Network [42]	Ultrasonic image	Classification of weld defects	Not specified	85.2
Random Forest [43]	Dynamic resistance signals	Classification according to weld quality	Resistance spot welding	93.6
Support Vector Machine [44]	3D shape from SFS algorithm	Detection of weld quality	Gas metal arc welding	94
Back propagation neural network [45]	Weld image from CCD camera	Classification of defects	Gas metal arc welding	95
Artificial neural network [46]	Parameters	Fault detection of welds	Remote laser welding	97.2

2 Experimental procedure

The bead-on-plate and V-groove welds were conducted using Kuka KR 16 robot gas metal arc welding with Fronius (TPS 5000) powersource. The specimens were flat plates with 12 mm thickness and v-grooved plates with 6 mm thickness made of SA 516 grade 70 material, which is used widely in pressure vessels. The shielding gas required for GMAW comprised the mixture of Argon and Carbon Dioxide gas with 80:20 proportion. The specimen was held firmly using a rigid fixture. The data acquisition system with a hall effect sensor and low pass filter were connected to acquire welding current and welding voltage respectively; the data acquisition rate was 8 kHz. The current and voltage data were recorded for each of the welds.

The stickout distance (SD), travel speed (TS), and gas flow rate (GR) were altered in each trial for examining the weld quality upon different welding parameters. The weld quality of the bead-on-plate trials was assessed by visual inspection and the control chart. Welding voltage-based control charts are proven to distinguish the welding quality. Three consecutive sample points outside the control limit indicate the arc instability and presence of porosity. The initial and the final sample point are insignificant and thereby can be avoided for quality inspection [13].

Control charts are plotted with a subgroup size of 4650 using Minitab software.

The quality of the welding that has been categorized as defect-free and defected weld is the output fed to the neural network. The input data to the neural network was tabulated from the statistical description of the voltage data (mean, standard error, median, mode, standard deviation, sample variance, kurtosis, skewness, minimum and maximum) for the bead-on-plate welds (19 different welds). The bead-on-plate welds conducted are shown in Fig. 1. The corresponding set of parameters, input and output data for training are given in Table 2. The 70%, 15% and 15% of the total input data were trained (13 samples), validated (3 samples) and tested (3 samples). When 70% of the data are used for training, the next 15% are used primarily for validating that the network is generalizing and terminating the training before overfitting. The remaining 15% is used for testing the network. The network has been set for testing after obtaining the perfect fit in the training process using bead-on-plate trial welds. For testing of ANN, twenty-two sets of V-groove plates were welded and the prediction capability of the network on quality was investigated. The test data comprises the voltage statistical description of these twenty-two v-groove welds. Twenty combinations of parameters for V-groove welds

Fig. 1 Bead-on-plate trial welds from 1 to 19 using gas metal arc welding process

are obtained from central composite design (3 factor and 2 level system) using Minitab software. High and low level of three parameters are given in Table 3 and the v-groove welds for the experimental runs with a different combination of parameters are listed in Table 4. Among twenty set of parameters, a combination of parameters—SD: 20 mm; TS: 50 cm/min; GR: 12 lpm are repeated six times according to central composite design. To investigate the influence of defect on the arc stability, four weld lines corresponding to parameters (SD: 20 mm; TS: 50 cm/min; GR: 12 lpm) and additional two welds with the same parameters have been applied with pinches of grease. These welds were observed to have porosities. The input and output of the test data is provided in Table 5. The predicted results and the actual weld quality were compared for determining the neural network identification rate. A representative workflow of the experimentation is shown in Fig. 2.

3 Results and discussions

The model with 10 inputs, one hidden layer with 10 neurons, an output layer with one neuron and one output was fixed by optimizing the classification accuracy in the confusion matrix for the prediction of weld quality. The functions such as 'trainscg' as a training function, tan-sigmoid, and softmax in the hidden layer and output layer

respectively are used for developing the two-layered feed-forward network. The schematic representation of the developed back propagation network (BPN) model is shown in Fig. 3. All the ten inputs to the neural network were found in literature to have an effect on the weld quality. A monitoring system with 95% identification rate to detect defected welds was suggested by Wu et al. [25] in which standard deviation, mean, kurtosis and coefficient of variance of voltage as well as mean, kurtosis and coefficient of variance of current were concluded to have a significant effect. This finding is validated in [23] stating that the standard deviation and mean of voltage in a control chart vary sensitively if there are imperfections like porosities in the weld. A main reason for this behaviour is due to the high sensitivity of current and voltage to the welding arc fluctuations. In gas metal arc welding with short arc transfer mode, an increase in the voltage was observed in voltage transients during arc disturbances. This proves the necessity of statistical parameter—'Maximum' in our study. Probability density distribution plotted using voltage and current signals were verified to have a unique pattern when burnthrough and porosity were artificially induced in gas metal arc welded joints [47]. All these studies evidently ascertain that the voltage variations in the powersource contain relevant information regarding the quality of the joints prepared using gas metal arc welding process. Therefore, 10 statistical parameters of voltage

Table 2 Statistical description of voltage data for the bead-on-plate trial welds

No.	SD	GR	TS	Mean	Standard error	Median	Mode	Standard deviation	Sample variance	Kurtosis	Skewness	Minimum	Maximum	Target
1	10	10	30	18.43295	0.021064	22.3	22.6	7.296886	53.24454	−0.64467	−1.06781	3.5	34.5	0
2	20	10	30	18.31879	0.018734	21.9	22.2	7.108978	50.53757	−0.8236	−0.96524	2.4	36	0
3	25	10	30	18.30908	0.017762	21	21.5	6.354839	40.38398	−0.54975	−1.02024	3.6	36.3	0
4	30	10	30	19.23385	0.020033	20.4	19.9	7.16718	51.36847	11.42771	1.421084	2.9	70.4	1
5	40	10	30	18.29725	0.018456	21.3	21.7	6.60315	43.60159	−0.61303	−1.02437	3	35.4	1
6	10	20	30	18.46904	0.019856	22.1	22.2	7.104071	50.46783	−0.43515	−1.14294	3.1	35.9	0
7	10	15	30	18.44034	0.019802	22	22.2	7.084445	50.18935	−0.51868	−1.10158	3.4	35.8	0
8	10	12	30	18.43459	0.020265	22.2	22.4	7.250396	52.56824	−0.57615	−1.09115	3.1	35.3	0
9	10	10	30	18.42891	0.020471	22.3	22.4	7.323795	53.63798	−0.61228	−1.08051	2.6	34.1	0
10	10	8	30	18.41421	0.019731	22.2	22.4	7.276364	52.94548	−0.63127	−1.07141	3	34.4	0
11	10	6	30	18.39619	0.02067	22.4	22.6	7.39524	54.68958	−0.7041	−1.03984	3.3	34.4	0
12	10	10	40	18.44651	0.022638	22.3	22.5	7.300608	53.29888	−0.6966	−1.00447	3.4	38.1	0
13	10	10	50	18.54291	0.032976	22.1	22.2	7.224751	52.19702	−0.36041	−1.18167	3.4	34	0
14	10	10	60	18.40747	0.03572	22	22.6	7.14407	51.03773	−0.32424	−1.20883	3.1	33.9	1
15	10	10	80	18.46675	0.025476	22.2	22.5	7.20588	51.9247	−0.41422	−1.16325	3.2	35.4	0
16	10	10	100	18.47056	0.030052	22.2	22.4	7.111775	50.57735	−0.46596	−1.15127	3.8	33.8	0
17	10	10	120	18.3964	0.022488	22.5	22.6	7.789978	60.68375	−0.88379	−0.93268	2.8	41.5	1
18	10	15	30	18.37228	0.026735	22.8	22.8	9.564954	91.48835	−0.99659	−0.36466	2.6	71.6	1
19	10	15	30	18.2875	0.022777	22.6	22.6	8.399803	70.5567	−1.04485	−0.74628	2.4	37.6	1

SD stick out distance, *GR* gas flow rate, *TS* travel speed

Table 3 High and low levels of parameters

Parameter	Low	High
Stick out distance (SD)	10	30
Gas flow rate (GR)	6	20
Travel speed (TS)	30	70

Table 4 Experimental runs (CCD) and V-groove welds

No.	SD	GR	TS	V-Groove welds	Weld Quality
1	10	6	30		Good quality
2	30	6	30		Porous weld
3	20	12	50		Good quality
4	36.8	12	50		Narrow bead width
5	10	6	70		Burn through
6	30	6	70		Porous weld
7	10	18	30		Good quality
8	10	18	70		Burn through
9	20	22.9	50		Good quality
10	20	1.9	30		Porous weld
11	30	18	30		Appreciable quality
12	30	18	70		Narrow irregular bead width
13	20	12	50		Good quality
14	8	12	50		Good quality
15	20	12	83		Burn through
16	20	12	16.3		Excessive reinforcement
17	20	12	50		Porous weld
18	20	12	50		Porous weld
19	20	12	50		Porous weld
20	20	12	50		Porous weld
21	20	12	50		Porous weld
22	20	12	50		Porous weld

data that are incorporated in this investigation are highly relevant for developing neural network model.

The training performance of the neural network model is shown in Fig. 4. The best validation performance is obtained at the 6th epoch having cross-entropy value equals 0.28854. The epoch is defined as the one forward pass and one backward pass of the entire training examples. It is affirmed that the cross-entropy value lying between 10^1 and 10^0 is

acceptable for the training of the data [48]. In fact, the epoch is the measure of a number of times that the complete training vectors are used to update the weights. There are various criteria for terminating the training process. This process stops when the maximum number of epochs is completed; maximum time is exceeded; performance is cut down to the goal; performance gradient falls below minimum gradient; moment exceeds the maximum moment, and when the validation performance increases with respect to last epoch continuously for more than the provided max_fail. Parameters for training scaled conjugate algorithm are given in Table 6. In this study, training of the input data was ceased when validation performance reached the max_fail. The cross-entropy of the training and testing are comparatively less than the validation at the 6th epoch. The validation process is used to avoid overfitting of the data. Validation accuracy of validation set has decreased continuously for six times after 6th epoch while the training accuracy was increased. This is an indication for the overfitting of the input data and is the reason for stopping the training process giving the best yield at 6th epoch. Therefore, weights leading to lowest cross-entropy at the sixth epoch is used for the neural network model. Achieved performance results herein are similar to a neural network developed for the purpose of predicting the welding parameters in which the training was also terminated with validation checks exceeding the limit [49].

The mean squared error and cross-entropy are mainly used to express the error between the calculated output and target output. The lower values of error are preferred for a better neural network model. However, the cross-entropy error is preferred over mean squared error for the classification and prediction since it contains categorical output (either 0 or 1). The cross-entropy error function is mathematically expressed for the binary classification as given in Eq. 1. i.e., it measures the difference between two probability distributions corresponding to actual and predicted. The log function in the cross-entropy error function helps in mathematically estimating the closeness of the prediction. In this study, 0 categorically represents quality welds and 1 as defected welds. Cross-entropy will be high if the predicted outcome is close to 1 but the actual outcome of the event is 0 and vice versa. This, in fact, represents the inaccuracy of the neural network model to predict the actual outcome. On the contrary, if actual and predicted outcome is the same or nearly close, it indicates the capability of the neural network model to predict the actual outcome accurately enhancing the identification rate.

$$\mathrm{Cross-entropy} = -(y \log(p) + (1-y) \log(1-p)) \quad (1)$$

where, y is the binary indicator or the actual outcome (0 or 1), p is the predicted outcome.

Table 5 Statistical description of voltage data for the test V groove welds

No.	SD	GR	TS	Mean	Standard error	Median	Mode	Standard deviation	Sample variance	Kurtosis	Skewness	Minimum	Maximum	Target
1	10	6	30	18.59364	0.017436	21.1	21.3	6.039876	36.4801	1.205036	−1.73012	3	32.7	0
2	30	6	30	20.75903	0.029761	21.1	19.9	10.64763	113.3721	6.832398	1.534659	2.4	74.3	1
3	20	12	50	18.47006	0.020892	20.3	20.3	5.285458	27.93607	2.456592	−2.04044	3.1	28.7	0
4	36.8	12	50	18.36565	0.019008	20.1	19.9	5.456231	29.77046	0.372741	−1.32305	4.1	32.8	1
5	10	6	70	18.6569	0.026212	20.1	20.2	4.689101	21.98767	4.750321	−2.49139	2.6	29.7	1
6	30	6	70	19.31523	0.038144	22.2	24.3	8.356979	69.83909	−1.01619	−0.62897	3.2	39	1
7	10	18	30	18.5437	0.017031	21.1	21	6.093174	37.12677	1.131304	−1.70557	2.9	32.9	0
8	10	18	70	18.60067	0.02472	20.2	20.2	4.943988	24.44302	3.610928	−2.28274	2.4	25.7	1
9	20	22.9	50	18.37534	0.023113	20.8	20.6	6.027197	36.32711	0.783225	−1.59471	3.2	30	0
10	20	1.9	30	19.45567	0.037518	24.6	4.7	10.61165	112.6071	−1.5252	−0.41292	2.7	39.3	1
11	30	18	30	18.28084	0.017108	20.9	21.3	6.308968	39.80307	−0.54623	−1.03139	4	35.1	0
12	30	18	70	18.30331	0.021726	20.1	19.9	5.496382	30.21021	0.407891	−1.35667	4.1	29.2	1
13	20	12	50	18.4287	0.020228	20.1	20.1	5.117281	26.18657	1.716346	−1.81433	3.1	29.2	0
14	8	12	50	18.57727	0.022116	20.9	20.9	5.934349	35.2165	1.535635	−1.8151	3.1	33.8	0
15	20	12	83	18.68312	0.036585	21	21	6.544695	42.83303	−0.10335	−0.95776	2.4	42.6	1
16	20	12	16.3	18.265	0.020068	22	22	7.179799	51.54952	−0.72877	−0.98241	2.4	40.6	1
17	20	12	50	27.23257	0.08364	21.9	74.1	21.15964	447.7305	0.570312	1.263776	2.5	74.9	1
18	20	12	50	18.25165	0.031342	21.7	21.3	7.928912	62.86765	−0.85289	−0.77669	2.8	56.7	1
19	20	12	50	18.27234	0.028551	21.4	21.9	7.222828	52.16924	−0.57902	−0.9797	2.9	36.2	1
20	20	12	50	18.27845	0.026802	21.3	21	6.780518	45.97543	−0.29842	−1.17548	2.5	36.9	1
21	20	12	50	18.28497	0.025269	20.8	20.6	6.392541	40.86458	0.018937	−1.27434	2.9	34	1
22	20	12	50	18.2738	0.028203	21.7	21.9	7.134987	50.90804	−0.59726	−1.05846	3	36.2	1

Fig. 2 Workflow of the experimental procedure
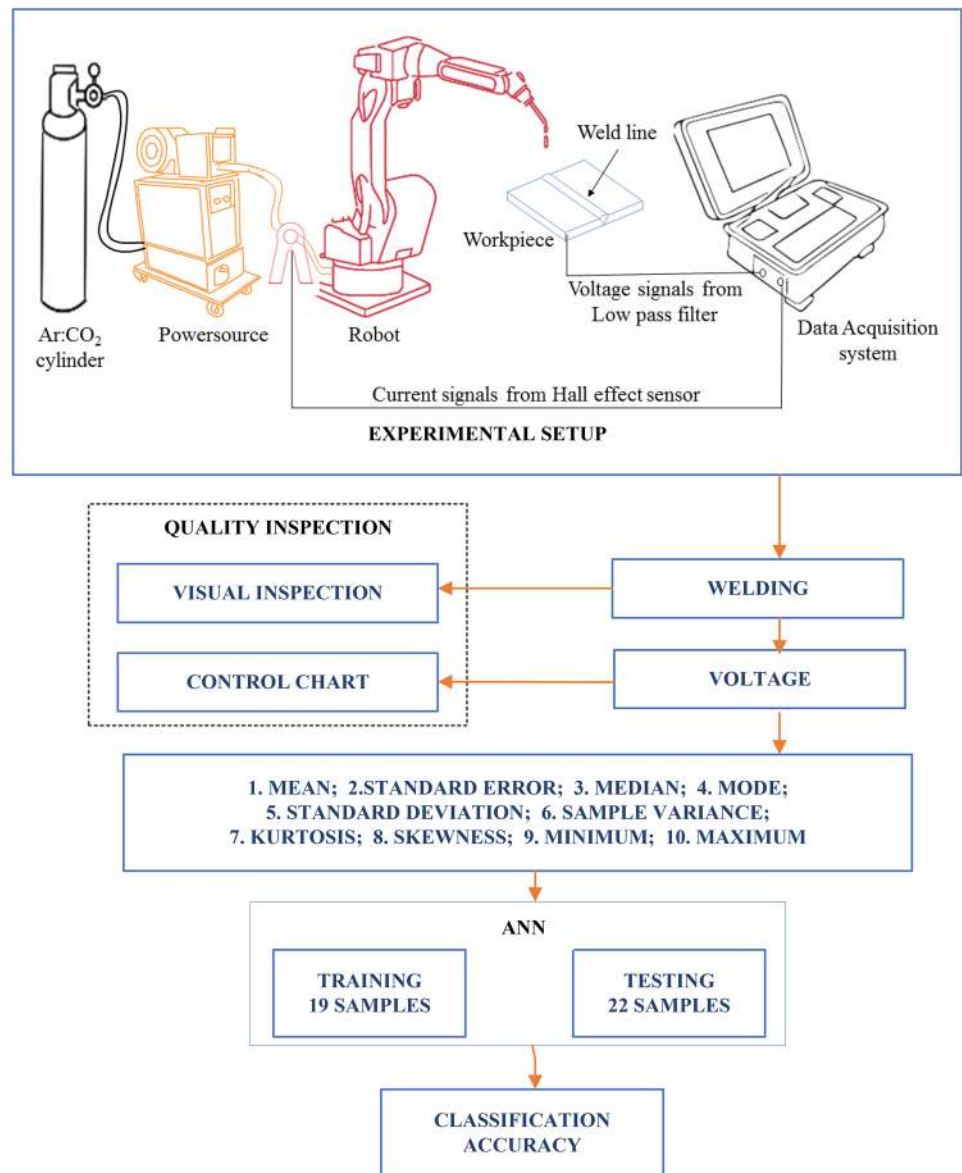
The gradient and the validation check at each of the epochs are shown in Fig. 5. The gradient at the 12th epoch was 0.11375. The initial gradient assigned at the start of the training process was 1. It is evident from the distribution of the validation checks that the training of the data was stopped when the validation check was increased six consecutive times. The gradient decreased slightly from 10^0 to a lower value. Lower the gradient, higher is the expected prediction rate.

The error histogram and the confusion matrices after the training process are shown in Figs. 6 and 7. It is worth to note that all of the data fitting errors except one were symmetrical to zero. I.e., errors are between the limits $(-0.4569, 0.404)$. However, the developed network failed to categorize one training data completely as the error noticed was 0.7115 which is very close to 1. As the target data is assigned as 0 and 1 for the quality and defected welds respectively, the test error equals 0.7115 is high. In this case, the ANN identified the quality weld as a defective weld. But in reality, the target assigned for the respective test weld was 0 as it was categorized as quality defect-free on visual inspection and control chart. The test confusion matrix proves that only one training data is incorrectly classified and hence is the reason for obtaining comparatively high cross entropy for training compared to testing as depicted in Fig. 4. In the case of testing and validation processes, all the corresponding data were correctly classified, and none were misclassified as seen in the confusion matrices. This is the reason for the testing and validation error to lie close to zero and symmetrical in the error histogram. The zero error implies that the target data and output data are nearly equal.
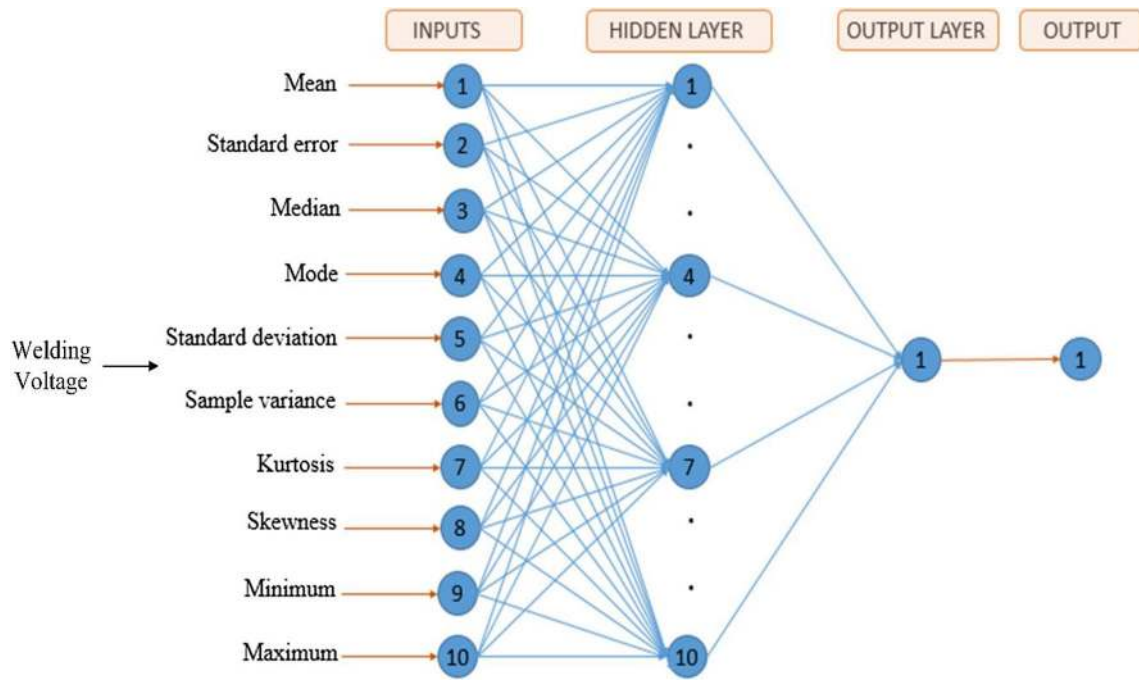
Fig. 3 Schematic representation of the BPNN model with statistical description of voltage as input and quality as output
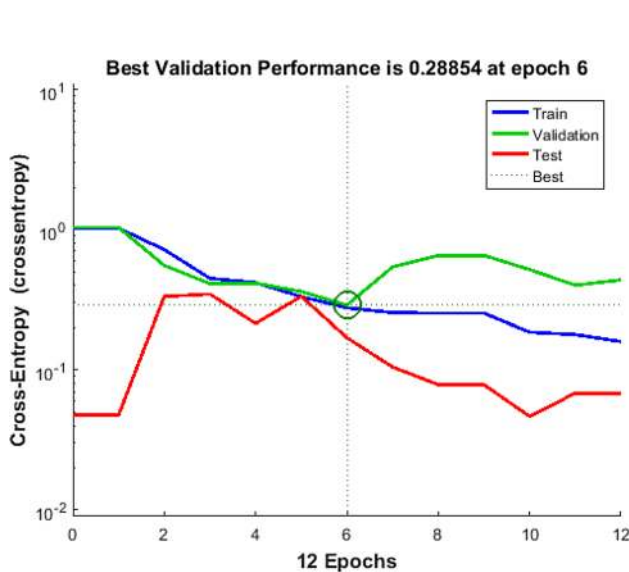
Fig. 4 Performance curve of the neural network

Fig. 5 Gradient and validation checks at each of the epochs

Table 6 Parameters used for training scaled conjugate algorithm

Maximum number of epochs	1000
Performance goal	0
Maximum time to train in seconds	Infinity
Minimum performance gradient	1.00E−06
Maximum validation failures	6

The classification accuracy of the training, testing and validation are 92.3%, 100% and 100% respectively. But, the overall classification accuracy of the neural network model for the known input and output was 94.7% ($18/19 \times 100$). The misclassification rate of the neural network model from the trained data was 5.3% which is very less. The sensitivity of the model to detect the defective welds was 100% ($5/5 \times 100$). The specificity of the model to detect the good quality welds was 92.85% ($13/14 \times 100$). The precision of the model to detect the defective welds was
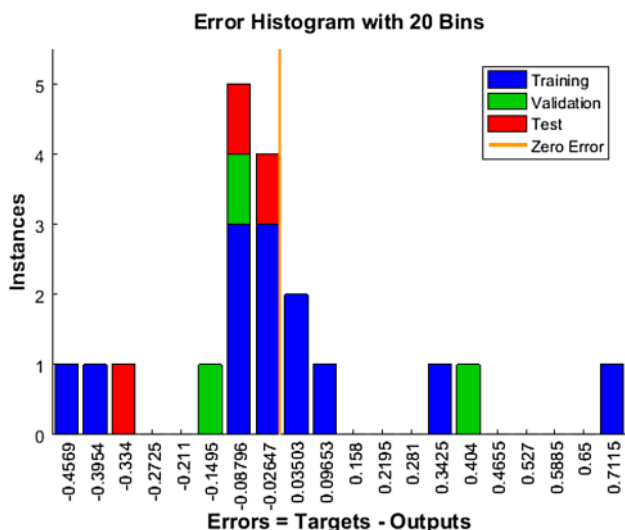
Fig. 6 Error histogram

83.3% (5/6 × 100). The prevalence of the model is 26.31% (5/19 × 100). Higher the classification accuracy, higher will be the identification rate. Since overall accuracy achieved in this investigation is 94.7% which is comparatively closer to the best classification accuracy levels (Table 1), the results are found to be satisfactory for the developed model.

A few other data mining algorithms were also analyzed preliminarily with the same bead-on-trial dataset to compare their classification accuracy with that of artificial neural network. Data mining algorithms such as decision tree, linear discriminant, logistic regression, quadratic support vector machine, cubic support vector machine, fine gaussian support vector machine, fine K-nearest neighbours were investigated. The classification accuracies obtained using the above algorithms are listed in Table 7. It is evident that the classification accuracies of these algorithms were comparatively low compared to that of artificial neural network. Among these, highest classification accuracy obtained is only 73.7% whereas that for ANN is 94.7%.

Fig. 7 Confusion matrix after training the bead-on-voltage voltage data

Table 7 Classification accuracy for algorithms using bead-on trial dataset

Data mining algorithms	Classification accuracy (%)
Fine tree	63.20
Linear discriminant	68.40
Logistic regression	63.20
Quadratic SVM	68.40
Cubic SVM	73.70
Fine gaussian SVM	68.40
Fine KNN	68.40

Henceforth, artificial neural network was selected as a best algorithm in this case for the weld quality inspection.

The whole purpose of training the developed model is to predict the quality of the weld from the fed data. However, the prediction capability with the testing data is assessed by comparing the known result with the predicted result. Quality of test v-groove joints is verified using visual inspection and control chart. Control charts were proved to identify defects and fluctuations in the arc stability. It has essentially two parts namely X-bar (Mean control chart) and S chart (standard deviation control chart) that are primarily used to reveal the variability of the process. Both of them have an upper control limit (UCL) and lower control limit (LCL). Control charts are plotted by categorizing the entire welding voltage data in such a way that each contains 4650 data. Mean and standard deviation of each of these 4650 data, hereafter called as sample points, are distributed in X-bar and S chart respectively. The process is considered to be unstable if the sample points are outside across any of the control limits and stable if they are within the control limits. The mean line in the X-bar and S chart statistically estimates mean voltage in the powersource and their standard deviation. In this research, this tool has shown unique characteristic in distinguishing defected and defect-free welds. Therefore, three each control charts of defected welds and quality welds among 22 set of test data are shown in Figs. 8 and 9 respectively. The voltage in the powersource and control chart were around 18.5 V corresponding to quality welds as in Fig. 9 indicating clearly that there are no voltage fluctuations. I.e., the estimated statistical mean voltage is close to set voltage in the powersource. On, the other hand, there was a rise in the voltage due to arc instability when porosities were created. Because of this fact, voltage has increased to more than 19 V owing to arc instability when porosities are formed as in Fig. 8. These extensive porosities were formed primarily due to inappropriate parameters. The lack of sufficient gas and higher stick-out-distances are the reasons for the formation of the porosity.

The higher stick-out-distance such as 30 mm and low gas flow rate of 1.9 lpm are inappropriate. Both of these extreme parameters reduce the shielding effect at the electrode deposition region causing atmospheric gases to be trapped in the weld region, leading to the formation of the porosity. For these reasons, the welds in Fig. 8a–c had porosities throughout the weld. The target data for these samples were assigned as 1 as shown in Table 4. But the control charts drawn for the defect-free v-groove welds (Fig. 9a–c) have their sample points inside the control limits except one or two in X-Bar and S-Chart. The stability of the process is assured if all the sample points are within the upper and lower limits. The initial sample point outside the control limit may be due to the lack of gas at the beginning of the weld. At the same time, the subgroup at the end may have less than 4650 data and therefore the sample point can be outside the control limit. In addition, the standard deviation of the 18th subgroup in 9(a), an 8th subgroup in 9(b) and 10th subgroup in 9(c) are outside the control limit indicating the chances for arc instability. However, the lack of three consecutive sample points outside the control limits proves these respective welds (see Fig. 9) to be defect-free welds. No defects identified in the respective welds experimentally validated the results from control charts. Since the location of the sample points in the control chart within or across the control limit reveals the quality of the weld, one or two sample points outside the control limit give a hint to the welder for cross-checking the welding parameters or welding conditions. This evidently proves that the welding voltage is sensitive to arc stability [47]. The arc disturbances have a major role in the creation of the defects. As the neural network model is investigated based on the voltage data, the control chart based on voltage is the most desirable to assign the desired or output target.

The confusion matrix after testing the test data is shown in Fig. 10. Twenty out of twenty-two test welds were correctly classified providing 90.9% classification accuracy. The misclassification accuracy is as low as 9.1%. It is worth to mention that the accuracy is satisfactory for a small data set. Compared to similar works as shown in Table 6, 90.9% classification accuracy is satisfactory for predicting the quality of the weld. This proves that the training of the bead-on-plate trial welds is sufficient for testing the v-groove welds.

The discussed method has many advantages which can be implemented in the welding industry. Generally, welders perform welding trials on a flat plate rather than on the real joints to check several aspects. The right selection of the electrodes, finding the right combination of parameters, checking adhesion of the molten electrode to the base material, to visualize bead geometry at different parameters, to analyze the suitability of welding positions
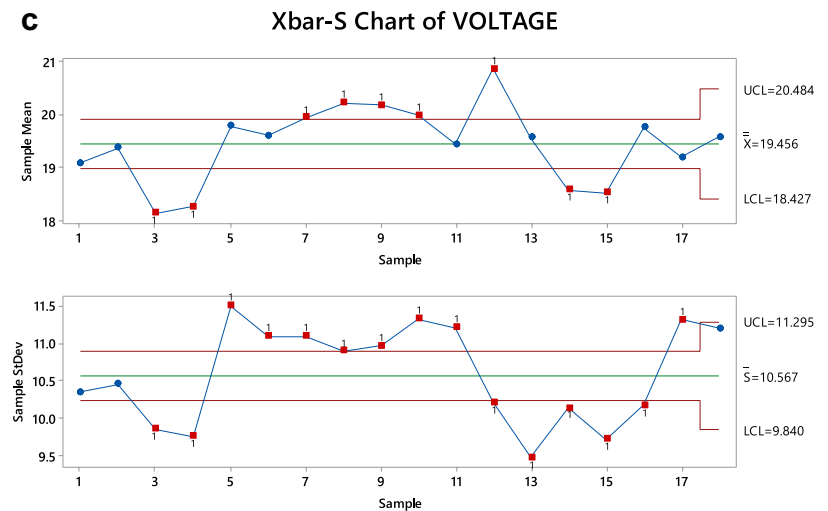
Fig. 8 Control chart of defected v-groove welds. **a** Stick out distance: 30; gas flow rate: 6; travel speed: 30. **b** Stick out distance: 30; gas flow rate: 6; travel speed: 70. **c** Stick out distance: 20; gas flow rate: 1.9; travel speed: 30
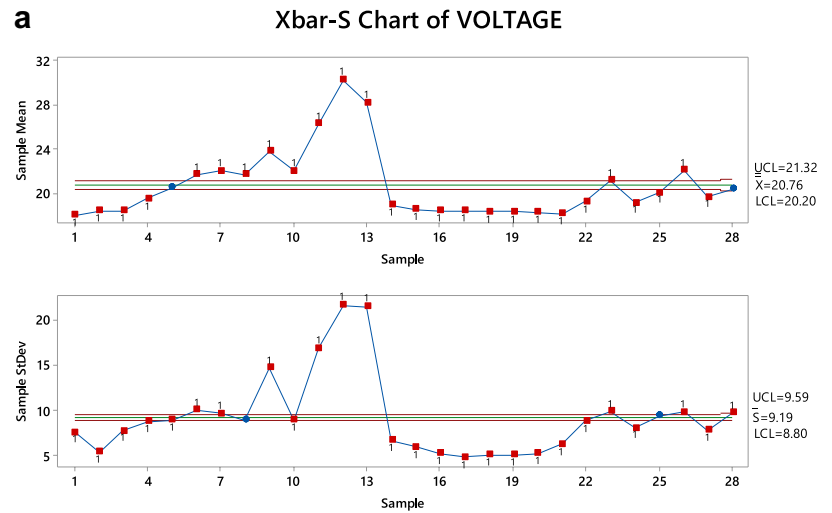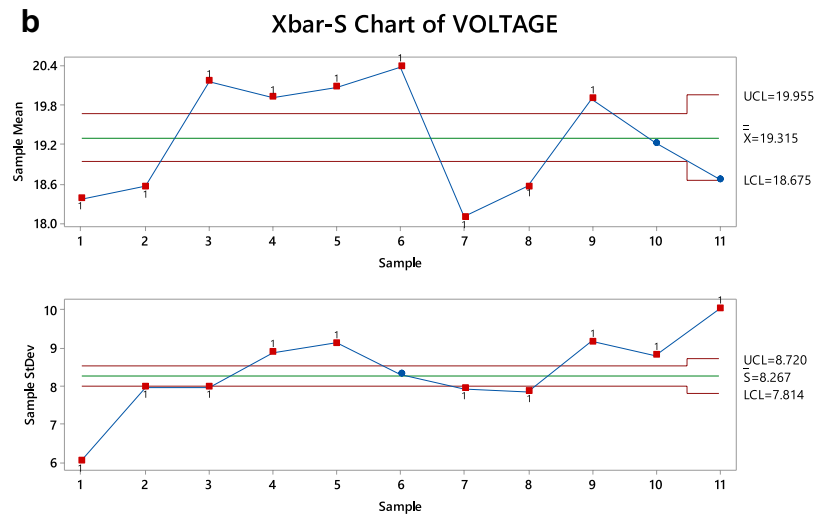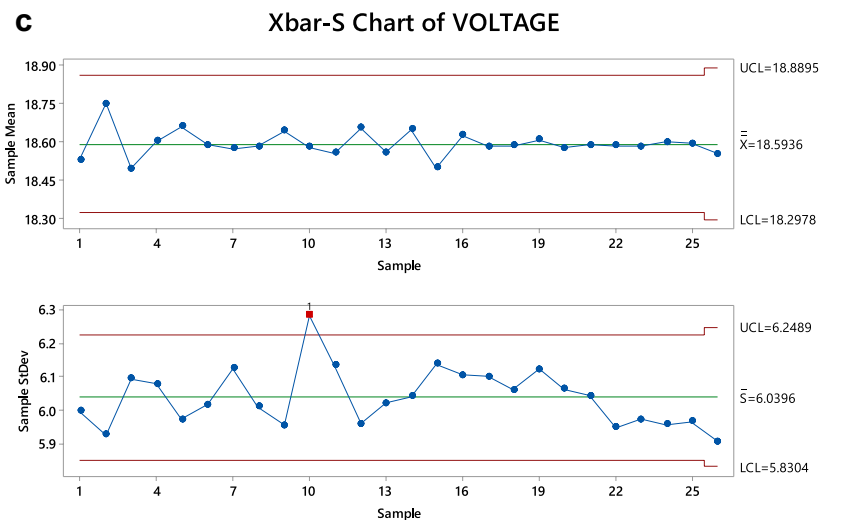
Fig. 9 Control chart of defect-free v-groove welds. **a** Stick out distance: 10; gas flow rate: 18; travel speed: 30. **b** Stick out distance: 20; gas flow rate: 12; travel speed: 50. **c** Stick out distance: 10; gas flow rate: 6; travel speed: 30
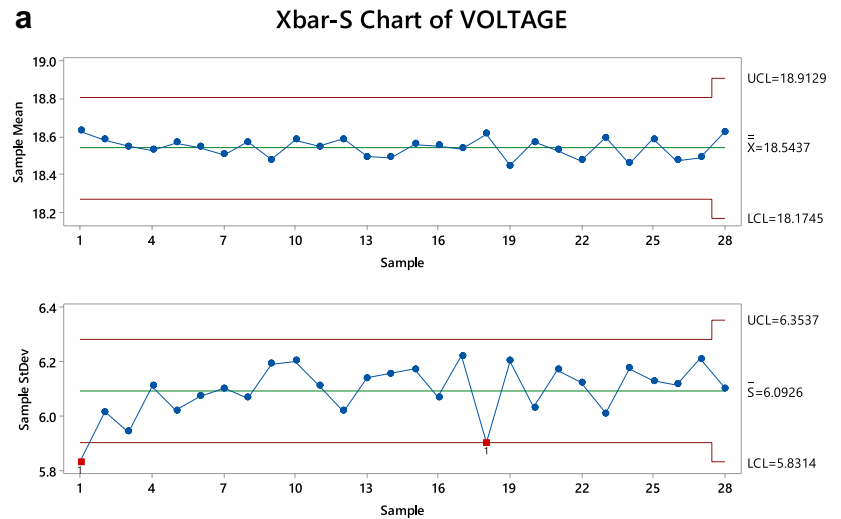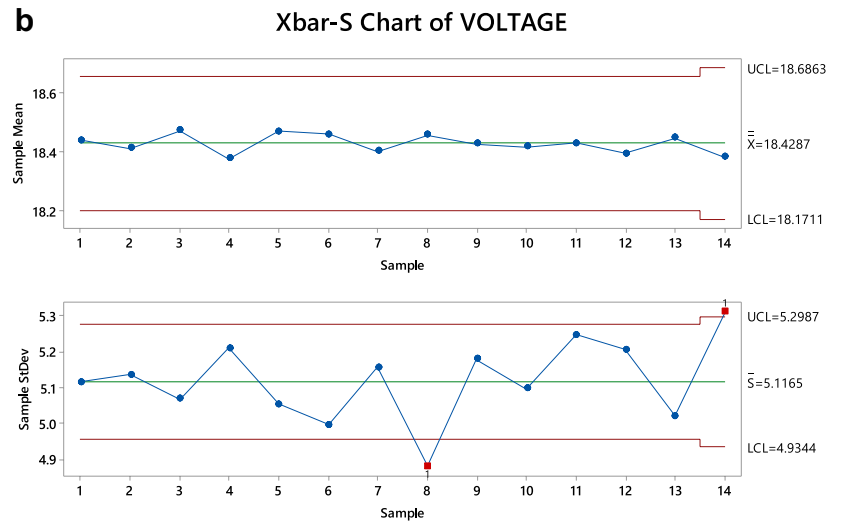
Fig. 10 Confusion matrix after testing the v groove welds

are some of the interests to perform bead-on-plate trial welds before producing actual weld joints. In our study, data collected using the bead-on-plate trial welds are used for testing V-groove welds. Therefore, enormous data can be collected from the trials following the procedure prescribed. Developed neural network and the approach are ideal for welders to set the optimum welding parameters for any material and geometry. Once the voltage from the powersource is captured using an appropriate data acquisition system, the data can be fed to the developed ANN for distinguishing quality and defect-free welds. The procedure is easy to use and highly reliable. Compared to conventional non-destructive tests, suggested ANN consumes less time and hence can be used for immediate estimation of the weld quality soon after the production of the weld joint. 90.9% accuracy rate of the proposed ANN developed with a small dataset is appreciable suiting for the current application. However, large data set after conducting the welding process extensively has to be prepared for better training and accuracy of the data. The suggested method, using ANN and acquired voltage data, are promising for the instantaneous inspection of the weld quality.

4 Conclusion

A voltage-based feed-forward back propagation network was developed for instantaneous inspection of the v-groove joint weld quality by conducting bead-on-plate trial welds using gas metal arc welding process. The effect of the three parameters; stick-out-distance, travel speed, and gas flow rate on weld quality was inspected using visual inspection and control charts. Classifiers such as decision tree, linear discriminant, logistic regression, quadratic support vector machine, cubic support vector machine, fine guassian support vector machine and fine K-nearest neighbours and artificial neural network were investigated initially with the bead-on-trial dataset. The classification accuracy obtained were 63.2%, 68.4%, 63.2%, 68.4%, 73.7%, 68.4%, 68.4% and 94.7% respectively. Therefore, artificial neural network was analyzed in the current study due to comparative high classification accuracy. The voltage data corresponding to the bead-on-plate and v-groove welds were selected for the training and testing process respectively. The training was terminated after reaching the validation fail for six consecutive times satisfying one of the stopping criteria. Out of 19 total data fed to the network, only one was misclassified during the training process. The accuracy for individual training, validation and testing obtained were 92.3%, 100% and 100% respectively. Thereby, the overall classification accuracy achieved was 94.7%. There was no evidence for the over-fitting and under-fitting of the data during the training process. The network with 5.3% misclassification accuracy and successful performance characteristics was set for testing the v-groove weld data. Out of twenty-two v-groove test data, twenty of them were correctly misclassified. Hence, the classification accuracy obtained for the testing data was 90.9%. The network presents a 9.1% misclassification accuracy for the data presented and this value is attributed because of only two misclassifications out of the twenty-two set of data. Any misclassification will lead to a considerable drop in accuracy if the data is very less. Therefore, it is recommended in the future to train a large data set after conducting numerous welding trials. However, the network is successful in distinguishing the weld quality condition of the v groove joints from bead-on-plate weld data. A comparative investigation of learning algorithms such as Levenberg–Marquardt, gradient descent and Bayesian regularization is in the future scope. The methodology using the artificial neural network and voltage data for each of the welds from the powersource is promising for a preliminary inspection of the weld quality condition.

Compliance with ethical standards

Conflict of interest On behalf of all authors, the corresponding author states that there is no conflict of interest.

References

1. Zhang Z, Chen X, Chen H et al (2014) Online welding quality monitoring based on feature extraction of arc voltage signal. Int J Adv Manuf Technol 70:1661–1671. https://doi.org/10.1007/s00170-013-5402-2

2. Feng S, Terasaki H, Komizo Y et al (2014) Development of evaluation technique of GMAW welding quality based on statistical analysis. Chin J Mech Eng 27:1257–1263. https://doi.org/10.3901/CJME.2014.0718.120

3. Maiti SK, Kishore GK, Mourad A-HI (2008) Bilinear CTOD/CTOA scheme for characterisation of large range mode I and mixed mode stable crack growth through AISI 4340 steel. Nucl Eng Des 238:3175–3185

4. Maiti SK, Mourad A-HI (1995) Criterion for mixed mode stable crack growth—II. Compact tension geometry with and without stiffener. Eng Fract Mech 52:349–378

5. Maiti SK, Namdeo S, Mourad A-HI (2008) A scheme for finite element analysis of mode I and mixed mode stable crack growth and a case study with AISI 4340 steel. Nucl Eng Des 238:787–800

6. Mourad A-HI, Alghafri MJ, Zeid OAA, Maiti SK (2005) Experimental investigation on ductile stable crack growth emanating from wire-cut notch in AISI 4340 steel. Nucl Eng Des 235:637–647

7. Chen S, Sun T, Jiang X et al (2016) Online monitoring and evaluation of the weld quality of resistance spot welded titanium alloy. J Manuf Process 23:183–191. https://doi.org/10.1016/j.jmapro.2016.06.003

8. Chu HH, Wang ZY (2017) A study on welding quality inspection system for shell-tube heat exchanger based on machine vision. Int J Precis Eng Manuf 18:825–834. https://doi.org/10.1007/s12541-017-0098-0

9. Li L, Xiao L, Liao H et al (2017) Welding quality monitoring of high frequency straight seam pipe based on image feature. J Mater Process Technol 246:285–290. https://doi.org/10.1016/j.jmatprotec.2017.03.031

10. Wan X, Wang Y, Zhao D et al (2017) Weld quality monitoring research in small scale resistance spot welding by dynamic resistance and neural network. Measurement 99:120–127. https://doi.org/10.1016/j.measurement.2016.12.010

11. Buffa G, Campanella D, Pellegrino S, Fratini L (2016) Weld quality prediction in linear friction welding of AA6082-T6 through an integrated numerical tool. J Mater Process Technol 231:389–396. https://doi.org/10.1016/j.jmatprotec.2016.01.012

12. Mourad A-HI, Khourshid A, Sharef T (2012) Gas tungsten arc and laser beam welding processes effects on duplex stainless steel 2205 properties. Mater Sci Eng A 549:105–113. https://doi.org/10.1016/j.msea.2012.04.012

13. Mourad A-HI, Harib KH, El-Domiaty A (2010) Fracture behavior of friction stir spot welded joint. In: ASME 2010 pressure vessels and piping division/K-PVP conference. American Society of Mechanical Engineers, pp 205–215

14. Mourad A-HI, Allam M, El Domiaty A (2014) Study on the mechanical behavior of aluminum alloy 5083 friction stir welded joint. In: ASME 2014 pressure vessels and piping conference. American Society of Mechanical Engineers, p V06AT06A014-V06AT06A014

15. Mourad A-HI, Maiti SK (1996) Mode II stable crack growth. Fatigue Fract Eng Mater Struct 19:75–84

16. Mourad A-HI, Maiti SK (1995) Influence of state of stress on mixed mode stable crack growth through D16AT aluminium alloy. Int J Fract 72:241–258

17. Mourad A-HI, El-Domiaty A, Chao YJ (2013) Fracture toughness prediction of low alloy steel as a function of specimen notch root radius and size constraints. Eng Fract Mech 103:79–93

18. Wan X, Wang Y, Zhao D (2016) Quality evaluation in small-scale resistance spot welding by electrode voltage recognition. Sci Technol Weld Join 21:358–365. https://doi.org/10.1080/13621718.2015.1115161

19. Subramaniam S, White DR, Jones JE, Lyons DW (1998) Analysis of arc voltage, current, and light signals in pulsed gas metal arc welding of aluminium. Sci Technol Weld Join 3:304–311. https://doi.org/10.1179/stw.1998.3.6.304

20. Ślązak B (2016) Analysis of instantaneous values of current and voltage parameters in the evaluation of process stability of shielded electrode welding. Weld Int 30:33–37. https://doi.org/10.1080/09507116.2014.937609

21. Pal S, Pal SK, Samantaray AK (2010) Prediction of the quality of pulsed metal inert gas welding using statistical parameters of arc signals in artificial neural network. Int J Comput Integr Manuf 23:453–465. https://doi.org/10.1080/09511922100 3667698

22. Thekkuden DT, Mourad A-HI, Christy JV, Idrisi AH (2018) Assessment of weld quality using control chart and frequency domain analysis. In: ASME 2018 pressure vessels and piping conference. American Society of Mechanical Engineers, p V06BT06A004-V06BT06A004

23. Thekkuden DT, Santhakumari A, Sumesh A et al (2018) Instant detection of porosity in gas metal arc welding by using probability density distribution and control chart. Int J Adv Manuf Technol. https://doi.org/10.1007/s00170-017-1484-6

24. Wei E, Farson D, Richardson R, Ludewig H (2001) Detection of weld surface porosity by statistical analysis of arc current in gas metal arc welding. J Manuf Process 3:50–59. https://doi.org/10.1016/S1526-6125(01)70033-3

25. Wu CS, Gao JQ, Hu JK (2007) Real-time sensing and monitoring in robotic gas metal arc welding. Meas Sci Technol 18:303–310. https://doi.org/10.1088/0957-0233/18/1/037

26. Dewan MW, Huggett DJ, Warren Liao T et al (2016) Prediction of tensile strength of friction stir weld joints with adaptive neuro-fuzzy inference system (ANFIS) and neural network. Mater Des 92:288–299. https://doi.org/10.1016/j.matdes.2015.12.005

27. Fazli Shahri HR, Mahdavinejad R (2018) Prediction of temperature and HAZ in thermal-based processes with Gaussian heat source by a hybrid GA-ANN model. Opt Laser Technol 99:363–373. https://doi.org/10.1016/j.optlastec.2017.09.024

28. Pavan Kumar N, Devarajan PK, Arungalai Vendan S, Shanmugam N (2017) Prediction of bead geometry in cold metal transfer welding using back propagation neural network. Int J Adv Manuf Technol 93:385–392. https://doi.org/10.1007/s00170-016-9562-8

29. Sarkar A, Dey P, Rai RN, Saha SC (2016) A comparative study of multiple regression analysis and back propagation neural network approaches on plain carbon steel in submerged-arc welding. Sadhana 41:549–559. https://doi.org/10.1007/s12046-016-0494-7

30. Møller MF (1993) A scaled conjugate gradient algorithm for fast supervised learning. Neural Netw 6:525–533

31. Castillo E, Guijarro-Berdiñas B, Fontenla-Romero O, Alonso-Betanzos A (2006) A very fast learning method for neural networks based on sensitivity analysis. J Mach Learn Res 7:1159–1182

32. Batra D (2014) Comparison between levenberg-marquardt and scaled conjugate gradient training algorithms for image compression using mlp. Int J Image Process (IJIP) 8:412

33. Mishra S, Prusty R, Hota PK (2015) Analysis of Levenberg–Marquardt and scaled conjugate gradient training algorithms for artificial neural network based LS and MMSE estimated channel equalizers. In: 2015 international conference on man and machine interfacing (MAMI). IEEE, pp 1–7

34. Baghirli O (2015) Comparison of Lavenberg–Marquardt, scaled conjugate gradient and Bayesian regularization backpropagation algorithms for multistep ahead wind speed forecasting using multilayer perceptron feedforward neural network

35. Gao J, Wu C, Hu J (2007) Real-time monitoring of abnormal conditions based on Fuzzy Kohonen clustering network in gas metal arc welding. Front Mater Sci Chin 1:134–139. https://doi.org/10.1007/s11706-007-0024-y

36. Sumesh A, Nair BB, Rameshkumar K et al (2018) Decision tree based weld defect classification using current and voltage signatures in GMAW process. Mater Today Proc 5:8354–8363. https://doi.org/10.1016/j.matpr.2017.11.528

37. Sumesh A, Thekkuden DT, Nair BB et al (2015) Acoustic signature based weld quality monitoring for SMAW Process using Data Mining Algorithms. Appl Mech Mater 813–814:1104–1113. https://doi.org/10.4028/www.scientific.net/AMM.813-814.1104

38. Sumesh A, Rameshkumar K, Mohandas K, Babu RS (2015) Use of machine learning algorithms for weld quality monitoring using acoustic signature. Procedia Comput Sci 50:316–322. https://doi.org/10.1016/j.procs.2015.04.042

39. Da Silva RR, Siqueira MHS, De Souza MPV et al (2005) Estimated accuracy of classification of defects detected in welded joints by radiographic tests. NDT E Int 38:335–343. https://doi.org/10.1016/j.ndteint.2004.10.007

40. Zapata J, Vilar R, Ruiz R (2011) Performance evaluation of an automatic inspection system of weld defects in radiographic images based on neuro-classifiers. Expert Syst Appl 38:8812–8824. https://doi.org/10.1016/j.eswa.2011.01.092

41. Carvalho AA, Rebello JMA, Sagrilo LVS et al (2006) MFL signals and artificial neural networks applied to detection and classification of pipe weld defects. NDT E Int 39:661–667. https://doi.org/10.1016/j.ndteint.2006.04.003

42. Theresa Cenate CF, Sangeetha DN, Ramadevi R et al (2016) Optimization of the cascade feed forward back propagation network for defect classification in ultrasonic images. Russ J Nondestruct Test 52:557–568. https://doi.org/10.1134/s106183091610003x

43. Xing B, Xiao Y, Qin QH, Cui H (2018) Quality assessment of resistance spot welding process based on dynamic resistance signal and random forest based. Int J Adv Manuf Technol 94:327–339. https://doi.org/10.1007/s00170-017-0889-6

44. Yang L, Li E, Long T et al (2018) A welding quality detection method for arc welding robot based on 3D reconstruction with SFS algorithm. Int J Adv Manuf Technol 94:1209–1220. https://doi.org/10.1007/s00170-017-0991-9

45. Senthil Kumar G, Natarajan U, Ananthan SS (2012) Vision inspection system for the identification and classification of defects in MIG welding joints. Int J Adv Manuf Technol 61:923–933. https://doi.org/10.1007/s00170-011-3770-z

46. Kurniadi KA, Ryu K, Kim D (2014) Real-time parameter adjustment and fault detection of remote laser welding by using ANN. Int J Precis Eng Manuf 15:979–987. https://doi.org/10.1007/s12541-014-0425-7

47. Sumesh A, Rameshkumar K, Raja A et al (2017) Establishing correlation between current and voltage signatures of the arc and weld defects in GMAW process. Arab J Sci Eng. https://doi.org/10.1007/s13369-017-2609-9

48. Akter T, Desai S (2018) Developing a predictive model for nanoimprint lithography using artificial neural networks. Mater Des 160:836–848. https://doi.org/10.1016/j.matdes.2018.10.005

49. Las-Casas MS, de Ávila TLD, Bracarense AQ, Lima EJ (2018) Weld parameter prediction using artificial neural network: FN and geometric parameter prediction of austenitic stainless steel welds. J Braz Soc Mech Sci Eng. https://doi.org/10.1007/s40430-017-0928-0